Microstructure of Carbon Nanofiber/Thermotropic Liquid Crystalline Polymer Composites

Sungho Lee, Amod A. Ogale

Department of Chemical and Biomolecular Engineering and Center for Advanced Engineering Fibers and Films, Clemson University, Clemson, South Carolina 29634-0909

ABSTRACT: The properties and microstructure of a thermotropic liquid crystalline polymer (TLCP, Vectran V400P) were investigated in the presence of carbon nanofibers (CNF). The electrical conductivity of TLCP increased with an addition of CNFs. The thermal analysis of pure TLCP and its composites revealed that a glass transition at $\sim 110°C$ did not change significantly. However, a decrease of tensile modulus and strength was observed with the addition of CNFs. WAXD studies showed a decrease of Herman's orientation parameter, indicating reduction of anisotropy of TLCP. Further, the disruption of molecular orientation of TLCPs was inferred by SEM and TEM analysis. SEM micrographs revealed a fibrillar structure for pure TLCPs at a macro-scale (2–5 µm). However, this structure was not observed in composites at the same scale even though micro-size fibrils (0.05 µm) were found with the addition of CNFs. TEM micrographs displayed banded structures of pure TLCPs, but these structures were not significant in the vicinity of CNFs. These observations confirmed that a decrease of molecular alignment and disruption of fibrillar structure of TLCP, in the presence of nanofibers, are attributed to a significant decrease in tensile modulus and strength. © 2009 Wiley Periodicals, Inc. J Appl Polym Sci 113: 2872–2880, 2009

Key words: thermotropic liquid crystalline polymers; nanocomposites; x-ray diffraction; TEM

INTRODUCTION

It is known that thermotropic liquid crystalline polymers (TLCPs) form highly oriented fibrils in the flow direction during processing because of the semi-rigid nature of the TLCP molecules, coupled with weak intermolecular interactions.[1] This structural feature results in excellent mechanical properties.[2] In addition, TLCPs have been attractive because of their thermal stability, chemical and flame resistance, low oxygen/water vapor permeability, processibility with low melt viscosity.[2–5] Those unique properties allowed TLCPs to have potential to apply in electrical and electronic components, apparatus for chemical processes, medical equipment, and aerospace industry.

However, like other polymers, TLCPs are not electrically conductive. Therefore, pure TLCPs are inadequate for sensitive electronics packaging applications that need electrostatic dissipative characteristics. Therefore, carbonaceous materials such as carbon blacks (CBs)[6–8], carbon fibers (CFs)[9,10], and carbon nanofibers (CNFs)[11,12] have been incorporated into TLCPs as conductive fillers. The goal of most of these literature studies was to enhance conductivity and evaluate EMI shielding effectiveness of TLCP composites.[6–12]

King et al.[8] incorporated CBs (Ketjenblack) into TLCP (Vectra A950, Ticona) using a twin screw extruder. Ketjenblack possesses a highly branched structure and a large surface area (1250 m²/g) compared to normal CBs, resulting in a significant decrease of electrical resistivity (10^{-2}–10^{-1} Ω cm)[8]. They found an electrical percolation threshold at 5 wt % of CB and volume resistivity decreased significantly down to 10^7 Ω cm. Other researchers reported that a similar CB content was required to observe percolation threshold phenomena.[10] We also reported a volume resistivity of 2×10^7 Ω cm with TLCP (Vectran V400P, Ticona) composites containing 5 wt % CNFs.[12]

Sawyer and Jaffe have described the microstructure of TLCPs, which were copolyester TLCPs composed of 2,6-naphthyly and 1,4-phenyl units.[13] They observed a fibrillar structure in the longitudinal direction. Fibrillar structure was described as a structure that is fiber-like with high aspect ratio, but does not possess fiber symmetry. Further, they observed tape-like structures, which are uniaxially oriented sheets. According to the hierarchical model,[13] TLCPs possess bundles of macro fibrils (5 µm), fibrils (0.5 µm), and micro fibrils (0.05 µm), in decreasing order of their size.

In the present study, mechanical performance of CNF/TLCP composites was correlated with their

structure. Because of the small diameter of CNFs ($\sim$ 0.1 μm), such composites have potential application in micromoldings whose thickness is $\sim$ 25 μm for which conventional carbon fiber (diameter of $\sim$ 8 μm) can not be used. TLCPs in the presence of carbon nanofibers were processed by extrusion and electrical, thermal, and mechanical properties were investigated. To interpret the effect of CNF on the structure of TLCP, the morphological features of composites were analyzed by wide angle X-ray diffraction, scanning electron microscopy, and transmission electron microscopy.

EXPERIMENTAL

Materials and processing

A commercial grade of TLCP (Vectran V400P, Ticona, the technical polymers business of Celanese A. G.) was used throughout this study. Vectran V400P is a random copolyester primarily of 1,4-HBA and 4,6-HNA, but contains other comonomers that provide selected meta-linkages[14]; Table I displays its relevant properties.[15] PyrografIII[TM] PR-24-PS carbon nanofibers (CNFs) were provided by Applied Science, Inc. (Cedarville, OH), and relevant properties are summarized in Table II.[16,17]

A lab scale twin screw extruder with 19 mm of diameter and 24 : 1 L/D ratio (Model MP2015, APV Chemical Machinery, Saginaw, MI) was used for mixing of TLCP and CNFs (1, 5, and 10 wt %). Before mixing, all materials were vacuum dried at 110°C for 24 h. The temperature of four heating zones was 170, 200, 250, and 250°C. The screw rotation speed was 10 $\sim$ 15 rpm. Physically blended TLCP and CNFs were fed into the hopper of extruder. Subsequently, the extrudates from a die, which have a diameter of 2 mm, were fed into a pelletizer (Haake PP1 pelletizer, Karlsruhe, Germany). This extrusion process was repeated three times for ensuring uniformly dispersed CNFs in TLCP. All pellets were vacuum dried at 100°C for 24 h before further process. Pure TLCP without any CNFs were also processed under the same condition. These samples served as the control material.

A compression press (Carver model 30-12-2T, Wabash, IN) was used for processing of the polymeric pellets into molded samples using a rectangular mold cavity (150 $\times$ 14 $\times$ 0.3 mm^3). A

TABLE I
Properties of Ticona Vectran V400P[15]

Glass transition point	110°C
Melting point	Not observed
Density (23°C)	1.40 g/cc
Moisture absorption (23°C/50% RH)	0.03 wt %

TABLE II
Properties of Carbon Nanofibers[16,17]

Diameter (nm)	116 ± 46
Length (μm)	30–100
N$_2$ surface area (m^2/g)	35
Total pore volume (cm^3/g)	0.069
Bulk electrical resistivity (Ω cm)	0.33

compression temperature of 210°C, pressure of $\sim$ 4 MPa, and a holding time of $\sim$ 4 min was used for all of the molded samples. These conditions mimic those encountered in thermoforming processes that are used to produce packaging products.

TLCP and its composite pellets were extruded using a single screw extruder. A circular die of 1 mm diameter (L/D = 10) was used at an apparent shear rate of 500 s^{-1}. These shear rates were calculated with a throughput and a die diameter: $\dot{\gamma}_{wa} = 4Q/\pi R^3$. The temperature profile was 170, 200, 250, and 250°C in the feed, two metering sections, and die, respectively. Extrudates were not postdrawn, and their nominal diameter was $\sim$ 0.8 mm.

Characterization

The static decay time was measured at 25°C using a static decay meter (Model 406D, Electro-Tech Systems, Glenside, PA) to characterize the ability of molded plaques to dissipate an induced surface charge. The test method was based on the Federal Test Method 101C, Method 4046, and Military Specification Mil-B-81705B that require 99% of the induced charge to be dissipated in less than 2 s. The electrical measurements were conducted at two different voltages (10 and 100 V) to account for low and high resistances and corrected for the specimen geometry. Ten replicate specimens were used for all electrical measurements.

Thermal analysis was performed in a Perkin-Elmer differential scanning calorimeter (Pyris 1 DSC, Waltham, MA). Samples were heated to 300°C at a rate of 20°C/min and held at that temperature for 10 min to erase thermal history of samples. Subsequently, samples were cooled to 50°C at a rate of 20°C/min and then heated up to 300°C again at a rate of 20°C/min for studying the effect of nanofibers on the non-isothermal crystallization.

To measure the mechanical properties, the extrudates for pure TLCP and its composites containing 1, 5, and 10 wt % CNFs were prepared. The tensile properties of extrudates were measured using an ATS Universal Tensile Tester 900 (Butler, PA) at 25°C. The crosshead speed was 50 mm/min for all specimens. The tensile property of each extrudates was an average of the tensile data from at least eight specimens.

The orientation in pure TLCP and its composites was observed from the azimuthal intensity distribution of wide angle X-ray diffraction (WAXD, Rigaku Corp., Tokyo, Japan) patterns obtained from an Osmic Micromax CuK X-ray source with a collimator pinhole size of 0.3 mm. The distance from the sample to the detector was 10 cm. Diffracted patterns were captured on 2-D image plates, which were scanned using a Fuji BAS 1800 scanner. An exposure time of 20 min per image was utilized throughout the study. The Fraser-corrected WAXD diffractograms were analyzed using Polar® 2.6.5 software.

A Hitachi FE S-4800 SEM (Hitachi America, Pleasanton, CA) was used for observing the fractured surface of pure TLCP and its composites. Samples cryofractured under liquid nitrogen were applied for this morphology study. The specimens were coated with platinum using a sputter coater for 2 min. TEM-Hitachi H 9500 transmission electron microscope (TEM) were used for investigating crystalline structure of TLCP in pure and composite forms containing 10 wt % CNFs. After cryo-microtoming at $-50°C$, samples were dispensed on a formvar/carbon film-supported copper grid.

RESULTS AND DISCUSSION

Property characterization

Figure 1 displays mean values for volume resistivity of pure TLCP and its composites. At 5 wt % nanofiber content, a significant volume resistivity drop (over three orders of magnitudes) occurred, which corresponds to the onset of percolation. The composites with TLCP with nanofiber content above 5 wt % displayed a static decay time of less than 2 s for both positive and negative charges, indicating that the ma-
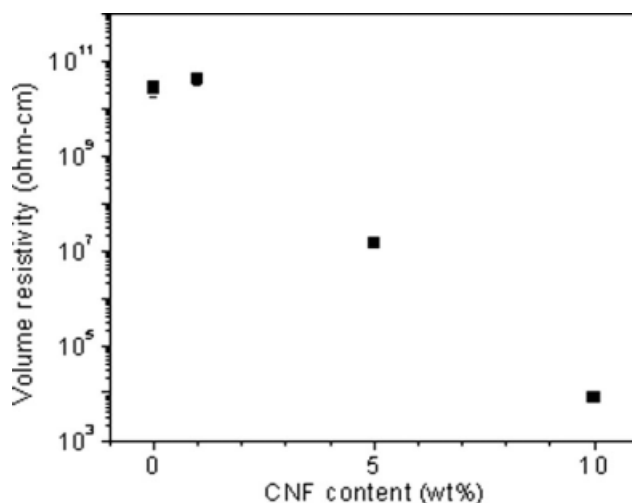
**Figure 1** Volume resistivity of pure TLCP and its composites.
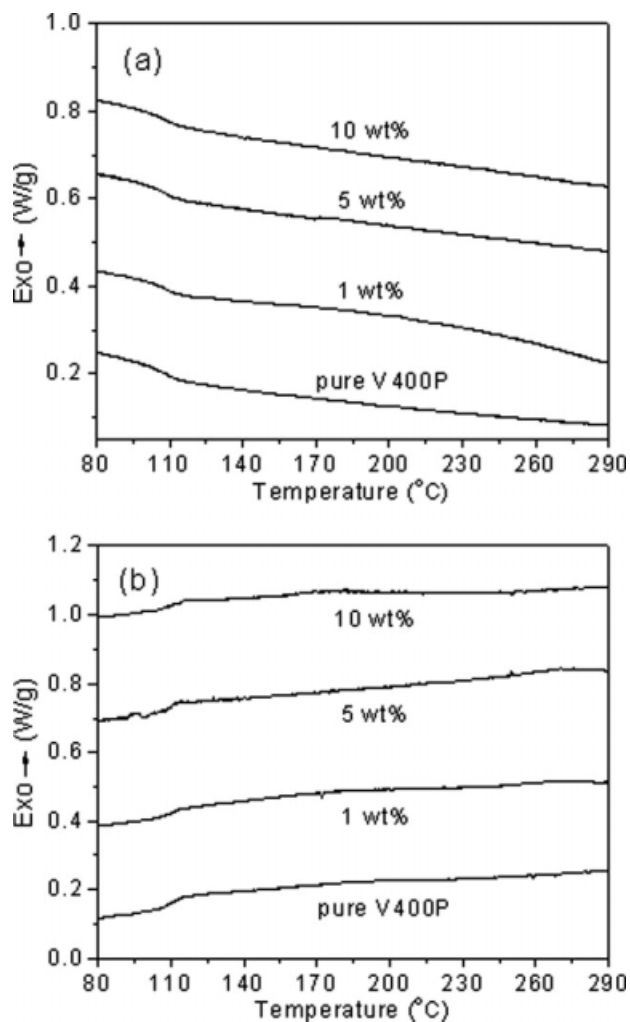
Figure 2 The DSC thermograms for pure TLCP and its composites for: (a) cooling at a rate of 20°C/min and (b) second heating a rate of 20°C/min.

terial is static dissipative at 5 wt % content of the nanofibers. Thus, this result confirmed that CNFs help an increase of electrical conductivity of TLCPs.

The thermal analysis of pure TLCP and its composites was conducted using non-isothermal DSC analysis. Baselines of all scans are shifted vertically for convenience. From Figure 2(a,b) for a cooling and the second heating scans, respectively, it is apparent that there is a glass transition at ~ 110°C with pure TLCP, but no melting or crystalline transitions and peaks during the heat up or cool down were observed. This indicates amorphous structure of TLCP, which is consistent with earlier studies.[5,14] It is interesting to note that all composites containing 1 to 10 wt % CNFs showed a single transition at ~ 110°C in DSC thermograms. This transition point did not change significantly with composition.

Tensile modulus and strength for extrudates of pure TLCP and its composites (1, 5, and 10 wt % of CNFs) are reported in Figure 3. There was no
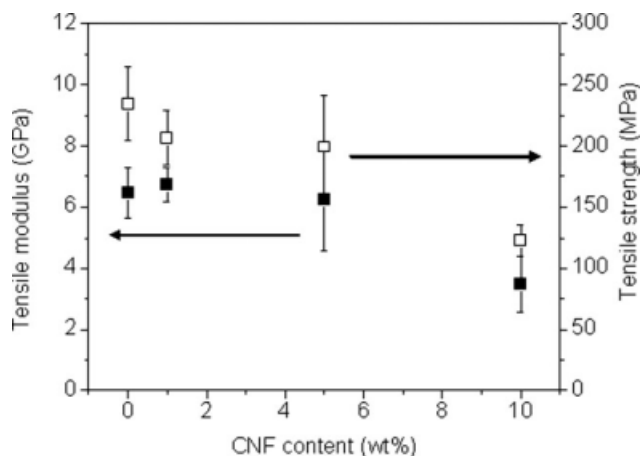
Figure 3 Tensile properties of pure TLCP and its composites. Solid and open squares are tensile modulus and strength, respectively. Error bars represent 95% confidence intervals.

statistically significant change in tensile modulus in going from pure TLCP to 5 wt % CNF composites. As the CNF content was increased up to 10 wt %,

tensile modulus surprisingly decreased significantly from ∼ 6.5 GPa to ∼ 3.5 GPa. For tensile strength, a small decrease was observed from pure TLCP (230 MPa) to 5 wt % CNF composites (200 MPa). However, 10 wt % composites revealed a significant drop of tensile strength to 120 MPa.

Wide angle x-ray diffraction analysis

WAXD analyses were performed for pure TLCP and its composites, which were extruded using a single screw extruder. Figure 4 displays individual 2D diffraction images of pure TLCP and its composites prepared at 500 s^{-1} of shear rate. For pure TLCP in integrated (2θ) intensity profiles [Fig. 5(a)], a distinct peak due to (110) planes at a 2θ of ∼ 19°, associated with pseudo-hexagonal packing of polymer chains, appeared.[18] It should be noted that the equatorial reflection is more intense for pure TLCP samples than for its composites. A shoulder also appeared in the 2θ of 26–28° due to (211) planes.[12] Addition of
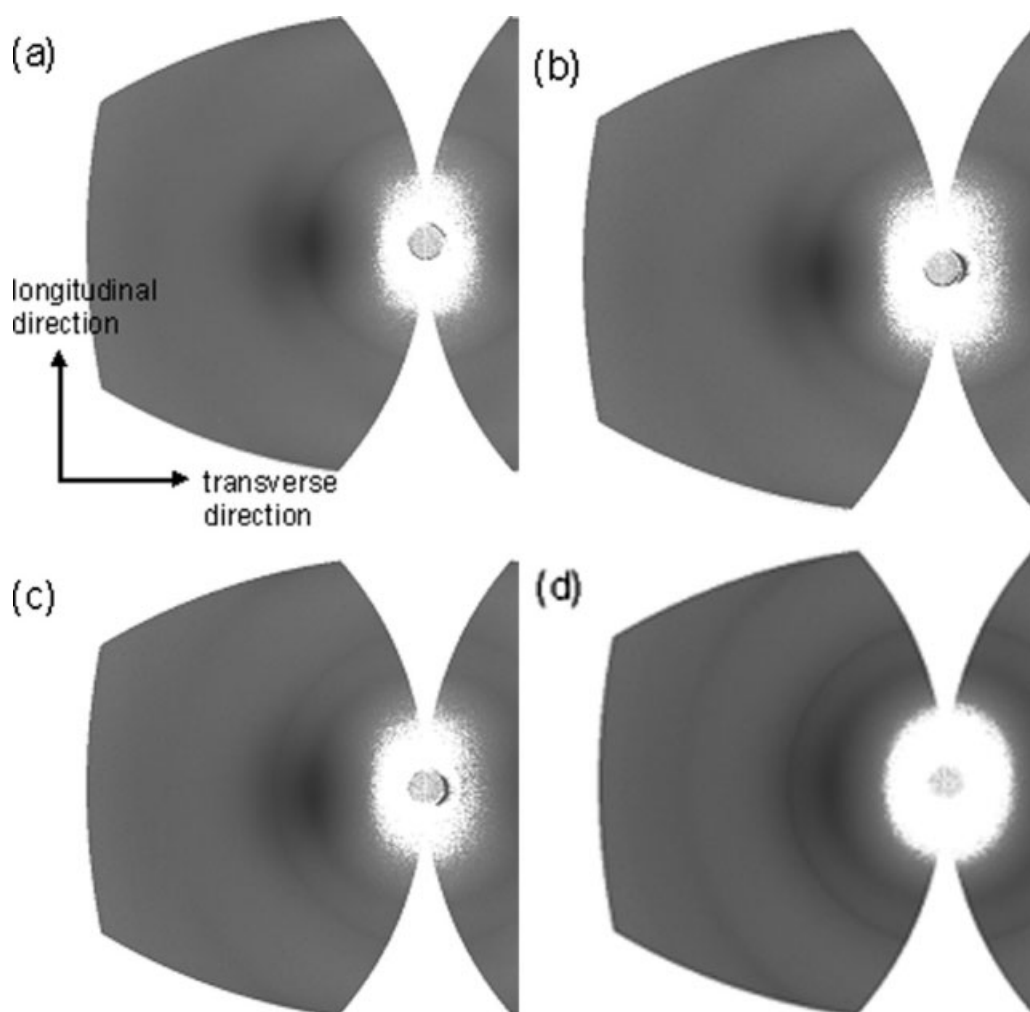
Figure 4 Wide angle x-ray diffraction patterns of extrudates: (a) pure TLCP, (b) 1 wt %, (c) 5 wt %, and (d) 10 wt % CNF composites.
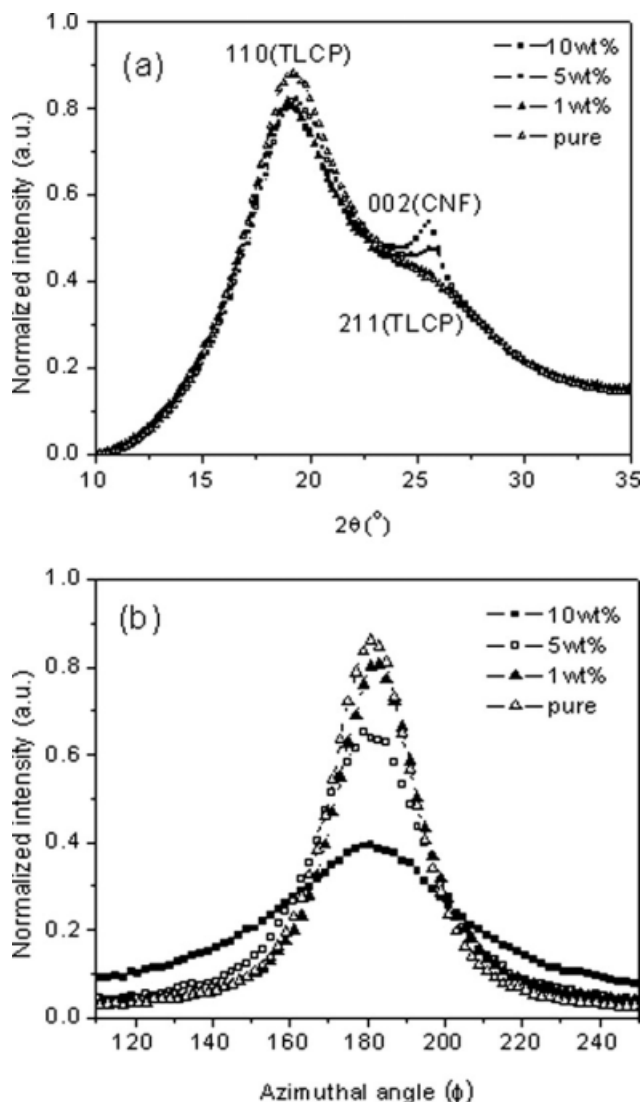
Figure 5 (a) Radial (2θ) intensity profiles and (b) azimuthal intensity profiles at $2\theta \sim 19°$ of extrudates: pure TLCP, 1 wt %, 5 wt %, and 10 wt % CNF composites.

CNFs into TLCP led to a reduction of the intensity of the equatorial peak and a uniform ring (Fig. 4). However, the (110) peak position of composites was same as that of pure TLCP [Fig. 5(a)]. Another intense peak at a 2θ of $\sim$ 26°, associated with graphene (002) planes from CNFs, was observed with 5 and 10 wt % composites. Normalized azimuthal intensity profiles at (110) peak are displayed in Figure 5(b). Higher contents of CNFs led to broader profiles, indicating that the orientation of TLCP chains becomes less severe with a gradual addition of CNFs.

Using the equatorial (110) peak, Herman's orientation parameter [$f = 0.5(3 < \cos^2\phi > -1)$] in the longitudinal direction was calculated for pure TLCP and its composites. Values were 0.86, 0.84, 0.80, and 0.74 for pure TLCP, 1 wt %, 5 wt %, and 10 wt % composites, respectively. From the f values, a signifi-

cant reduction of orientational structure of TLCP was observed, indicating that these results confirm that CNFs decrease molecular orientation of TLCPs.

Microstructure

Figure 6(a) displays a cross section of a pure TLCP sample cryo-fractured under liquid nitrogen at a low magnification (100×). It is interesting to note that the cross section was not circular, but was deformed. Various sheet-like structures appeared. It is likely that tensile force applied during testing, which can lead to a severe orientation in the longitudinal direction, led to these structures. In higher magnification SEM micrographs, additional features were observed. Figure 6(b) displays a typical fibrillar structure. Further, tape-like structure was observed in Figure 6(c). These are layered sheets made by aligned bundle of fibrils. In Figure 6(d), fibrils, having a diameter of 2–5 μm became tapered at the end, indicating necking resulting from tensile forces.

Figure 7(a–d) display cross-sections of composites containing 10 wt % of CNFs. Samples were prepared by cryo-fracturing in liquid nitrogen. From Figure 7(a), it is evident that the cross-section is circular and intact, in contrast to that for pure TLCP. Further, fibrillar and tape-like structures, which were observed for pure TLCP, did not appear to any appreciable extent [Figure 7(a,b)]. Therefore, it is inferred that the highly oriented structure along longitudinal direction, one of TLCP characteristics, was modified in the presence of CNFs. However, in higher magnification micrographs of composites [Figure 7(c,d)], micro fibrils (0.05 μm) of TLCP were observed even though their aspect ratio was not high. CNFs were distinguished by uniform diameter and hollow core, whereas TLCP fibrils were tapered at the end. It is evident that CNFs pulled out from TLCP matrix even though the other side of CNFs was wetted by the TLCP matrix.

These morphological changes confirm the effect of CNFs in disrupting the severe orientation that can otherwise develop in TLCPs. From WAXD results, it was confirmed that CNFs led to a reduction of the degree of orientation of TLCPs. SEM micrographs further confirm that macro-fibrillar structure of TLCPs was not significant in the presence of CNFs, even though micro-fibrillar structure existed. The fibrillar hierarchy has been also reported in prior literature studies.[13,19] Further, a decrease of molecular alignment and disruption of fibrillar structure of TLCP, in the presence of nanofibers, are attributed to a significant decrease in tensile modulus and strength (Fig. 3). It is noticed that addition of nanofibers prevents the TLCP matrix from forming a highly ordered structure, which reduces the anisotropy.
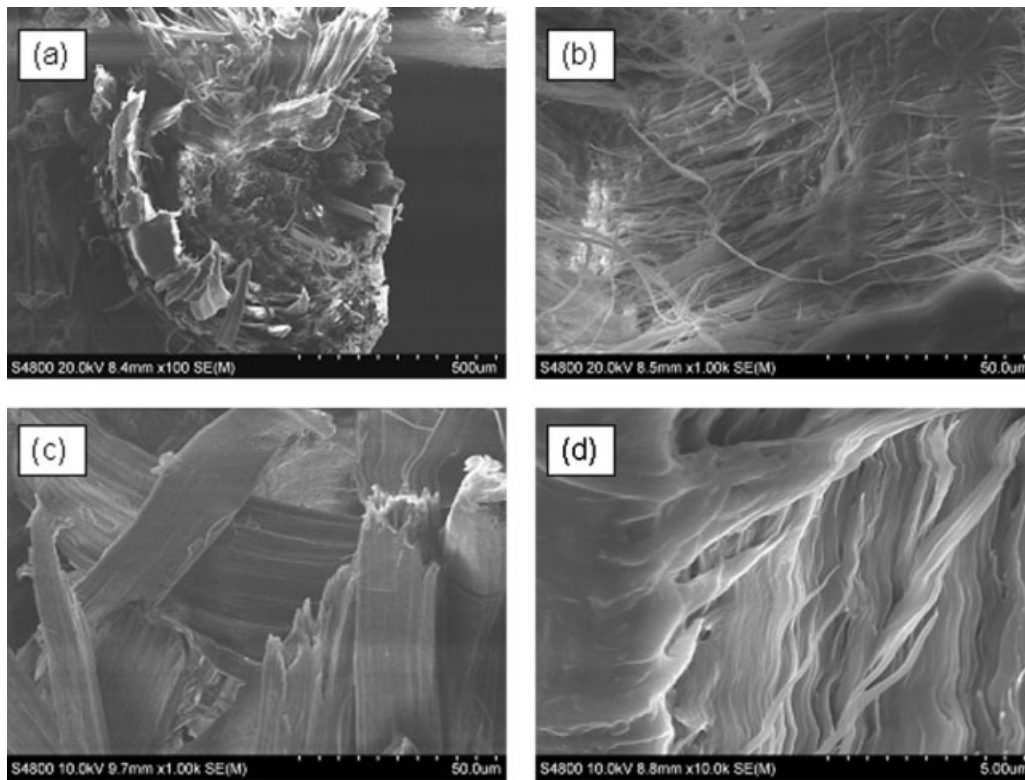
Figure 6   SEM micrographs of pure TLCP at various magnifications: (a) 100, (b) 1 K, (c) 1 K, and (d) 10 K.
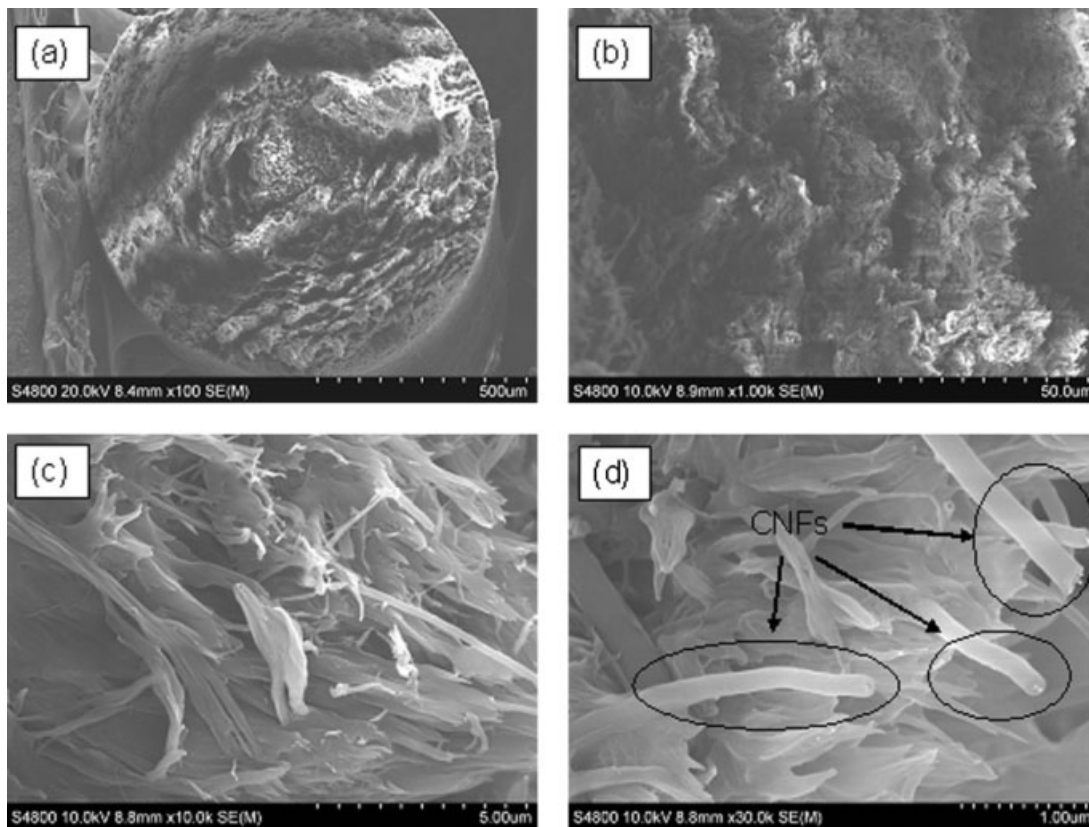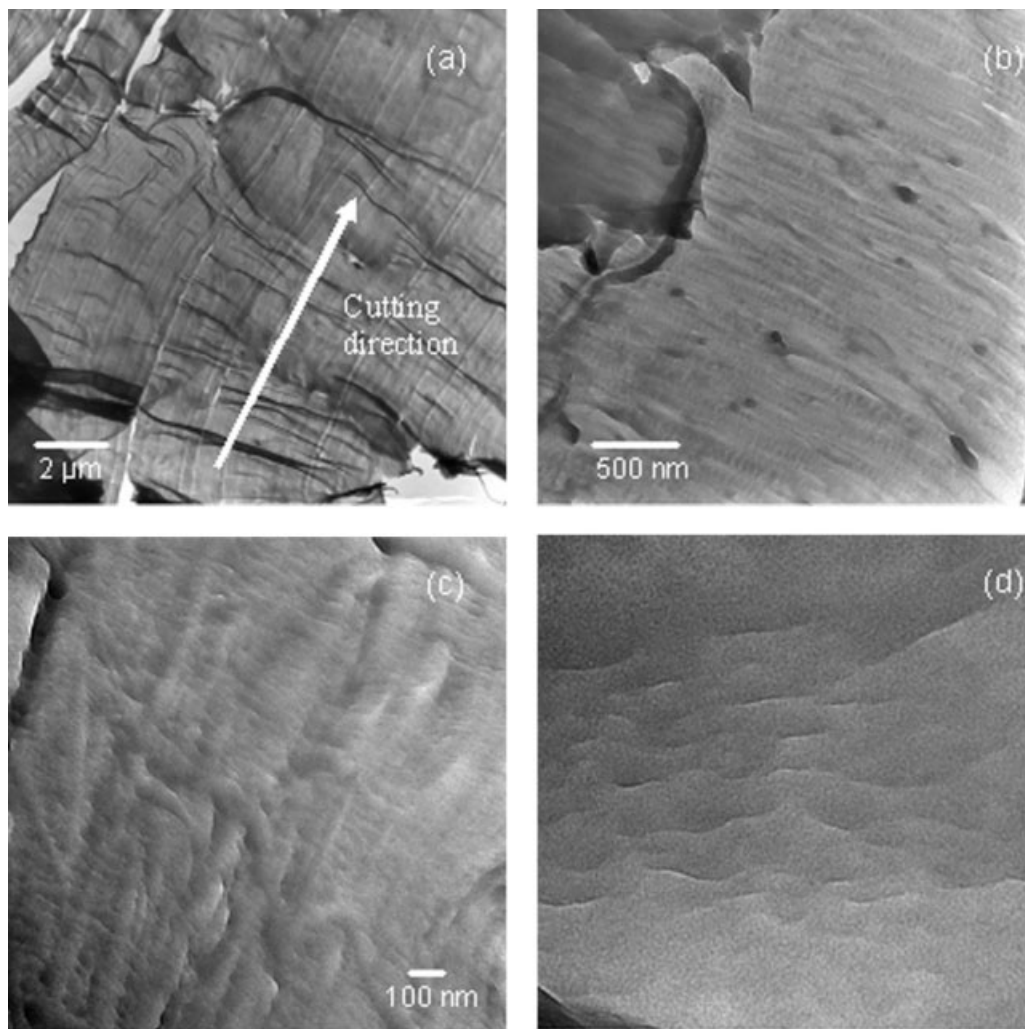

Figure 7   SEM micrographs of TLCP/10 wt% CNF at various magnifications: (a) 100, (b) 1 K, (c) 10 K, and (d) 20 K.

Figure 8 TEM micrographs of pure TLCP at various magnifications: (a) 10 K, (b) 50 K, (c) 100 K, and (d) 300 K.

For observing structure at higher magnification, transmission electron microscopy (TEM) analysis was performed. Extrudates of pure TLCPs and their 10 wt % CNF composites were cryo-microtomed in the perpendicular direction using a diamond knife under liquid nitrogen. Figure 8(a) displays bright field images for pure TLCP at low magnification. Contrast in bright field image of TEM results from thickness variation. Bright and dark sections indicate thin and thick regions, respectively. These are artifacts of cutting (white lines), which also resulted in folding of layers (black lines) perpendicular to longitudinal direction, as illustrated by the arrow on the micrographs in Figure 8(a).

It should be noted that at higher magnification, micrographs were obtained from relatively homogeneous areas to avoid artifacts noted above. In Figure 8(b), banded structures were observed even though they are small and weak. These are more significant in Figure 8(c), and finally very fine wavy structures appeared in Figure 8(d). Figure 8(d) indicates that

these microbands were observed in the present results as a wavy path of molecules. Width of the dark bands was 10–50 nm, which is relatively smaller than those from literature studies.

Microstructure of TLCPs has also been studied using other techniques such as scanning tunneling microscopy (STM)[19] and TEM.[13,19–23] From TEM micrographs, the most interesting feature of TLCPs was the banded structure which is associated with a serpentine path or "meander of the molecules" at a periodicity of 500 nm.[21] Donald et al. observed bands of alternating diffracting (bright) and non-diffracting (dark) regions.[20] Further, these bands were normal to the shear direction. In contrast, bright field imaging did not show clear banded structures. Banded structures of Vectra grade TLCPs have also been reported by other scientists.[13,19,22,23] Sawyer and Jaffe observed the periodicity of the microbands with a size of 100 nm from as-spun fibrils by TEM.[13]

Sawyer et al. confirmed periodic microbanded structures by STM, which is capable of imaging
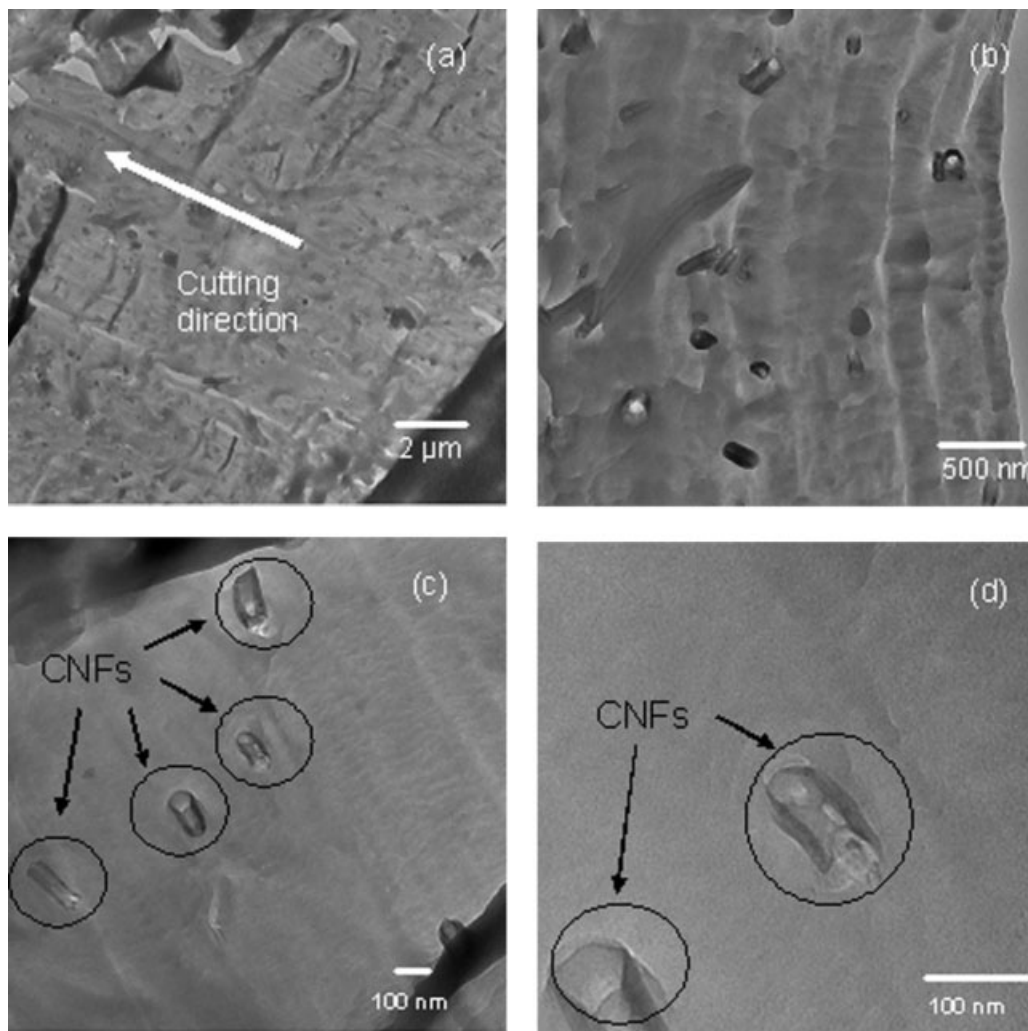
Figure 9 TEM micrographs of TLCP/10 wt% CNF at various magnifications: (a) 10 K, (b) 50 K, (c) 100 K, and (d) 300 K.

down to 1 nm. Further, three-dimensional images of Vectran fibers by STM revealed that microfibrils possessed tape-like structure with width of 10–50 nm and thickness of 2–10 nm rather than a round fibrous structure.[19] Using these observations, an expanded hierarchical fibrillar structure model with more detailed microfibril sizes, shapes, and order was suggested.[19] Because the TEM micrographs reported here are two-dimensional, information about thickness of microstructure cannot be obtained from Figure 8(d). However, width of dark bands (10–50 nm) is consistent with results from STM micrographs by Sawyer et al.[19]

TEM micrographs of composites containing 10 wt % CNF content are shown in Figure 9(a–d). Artifacts such as cutting lines and folding by microtoming appeared at a low magnification [Fig. 9(a)], which were also observed for pure TLCP. From Figure 9(b,c), it was evident that CNFs were fairly dispersed, but they are not oriented along one direction, indicating that the flow field applied for

sample preparation is not strong enough to align discontinuous CNFs in TLCP matrix. This may disrupt the anisotropy of TLCP. In Figure 9(c), several microbands were observed. However, Figure 9(d) suggests that microbands were not significantly observed in the vicinity of CNFs, indicating a disruption of periodicity of banded structures.

CONCLUSIONS

The electrical conductivity of thermotropic liquid crystalline polymer (TLCP) increased with an addition of CNFs. Thermal analysis revealed that the glass transition at $\sim 110°C$ did not change significantly with composition (1, 5, and 10 wt % of CNFs). This suggests an insignificant effect of CNFs on thermal behavior of TLCPs. However, a significant change of tensile modulus and strength was observed with an increase of CNF content. Tensile modulus and strength decreased from 6.5 GPa for pure TLCP to 3.5 GPa for 10 wt % CNF composites,

and from 230 MPa for pure TLCP to 120 MPa for 10 wt % CNF composites, respectively.

WAXD studies showed a decrease of Herman's orientation parameter from 0.86 for pure TLCP to 0.74 for 10 wt % CNF composites, indicating a reduction of anisotropy of TLCP. Further, the disruption of molecular orientation of TLCPs was inferred by SEM and TEM analysis. SEM micrographs revealed a fibrillar structure for pure TLCPs at a macro-scale (2–5 μm). However, this structure was not observed in composites at the same scale even though micro-size fibrils (0.05 μm) were found with the addition of CNFs. TEM micrographs displayed banded structures of pure TLCPs, but these structures were not significant in the vicinity of CNFs. These results indicate that CNFs can help to reduce the severe anisotropy that is otherwise observed for TLCPs. These observations confirmed that a decrease of molecular alignment and disruption of fibrillar structure of TLCP, in the presence of nanofibers, are attributed to a significant decrease in tensile modulus and strength.

References

1. Donald, A. M.; Windle, A. H. Liquid Crystalline Polymers; Cambridge University press: Cambridge, 1992.
2. Handlos, A. A.; Baird, D. G. Polym Comp 1996, 17, 73.
3. Chiou, J. S.; Paul, D. R. J Polym Sci A Polym Phys 1987, 25, 1699.
4. Foldberg, G.; Hedenqvist, M. S.; Gedde, U. W. Polym Eng Sci 2003, 43, 1044.
5. Guo, T.; Harrison, G. M.; Ogale, A. A. Polym Eng Sci 2005, 45, 187.
6. Wong, Y. W.; Lo, K. L.; Shin, F. G. J Appl Polym Sci 2001, 82, 1549.
7. Tchoudakov, R.; Narkis, M.; Siegmann, A. Polym Eng Sci 2004, 44, 528.
8. King, J. A.; Morrison, F. A.; Keith, J. M.; Miller, M. G.; Smith, R. C.; Cruz, M.; Neuhalfen, A. M.; Barton, R. L. J Appl Polym Sci 2006, 101, 2680.
9. Jou, W. S.; Wu, T. L.; Chiu, S. K.; Cheng, W. H. J Electron Mater 2001, 31, 178.
10. Wolf, H.; Willert-Porada, M. J Power Source 2006, 153, 41.
11. Yang, S.; Lozano, K.; Lomeli, A.; Foltz, H. D.; Jones, R. Compos Part A 2005, 36, 691.
12. Lee, S.; Kim, M. S.; Naskar, A. K.; Ogale, A. A. Polymer 2005, 46, 2663.
13. Sawyer, L. C.; Jaffe, M. J Mater Sci 1986, 21, 1897.
14. Linstid, H. C., III; Cangiano, D. L.; Demartino, R. N.; Kuder, J. E.; Provino, V. J.; Jester, R. U.S. Patent 6,294,640, 2001.
15. Ticona Vectran Liquid Crystal polymer (LCP) Product Information, Ticona, Summit, NJ, 07901: 2008.
16. Lee, S.; Kim, M. S.; Ogale, A. A. J Appl Polym Sci 2007, 106, 2605.
17. Lee, S.; Kim, T. R.; Ogale, A. A.; Kim, M. S. Synth Met 2007, 157, 644.
18. Sun, Z.; Cheng, H. M.; Blackwell, J. Macromolecules 1991, 24, 4162.
19. Sawyer, L. C.; Chen, R. T.; Jamieson, M. G.; Musselman, I. H.; Russell, P. E. J Mater Sci 1993, 28, 225.
20. Donald, A. M.; Windle, A. H. J Mater Sci 1983, 18, 1143.
21. Donald, A. M.; Viney, C.; Windle, A. H. Polymer 1983, 24, 155.
22. Taylor, J. E.; Romo-Uribe, A.; Libera, M. R. Polym Adv Technol 2003, 14, 595.
23. Chan, C. K.; Gao, P. Polymer 2005, 46, 10890.